

LOW NOISE HEMTs WITH MULTI - FEED GATE CONFIGURATIONS

K.Hosogi, T.Katoh, T.Kashiwa, H.Matsuoka, H.Minami, K.Kosaki,
K.Nagahama, K.Nishitani, and M.Otsubo

Optoelectronic and Microwave Devices R&D Laboratory
Mitsubishi Electric Corp.
4-1 Mizuhara, Itami, 664 Japan

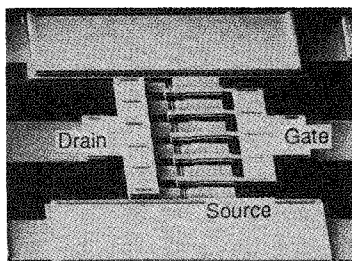
ABSTRACT

A novel multi-feed gate configuration using air-bridge metallization is demonstrated for low noise HEMTs. The configuration is designed according to the detailed analysis of parasitic gate capacitances. Very low noise figures of 0.55 and 1.6dB have been achieved at 12 and 40GHz for $0.25\mu\text{m}$ gate AlGaAs/InGaAs pseudomorphic HEMT, respectively. The noise figure of 4.1dB and the gain of 12.2dB at 40GHz are also obtained for the 2-stage HEMT MMICs.

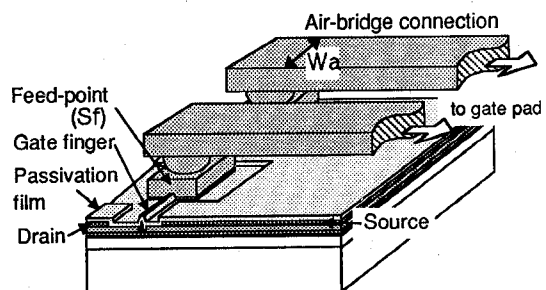
INTRODUCTION

The noise performances of HEMTs have been much improved by reducing gate length to quarter-micron or less[1,2]. T-shaped gates have been widely applied to the sub-quarter-micron gate HEMTs for reducing the gate resistance, which increases drastically with decreasing the gate length. However, in realizing the T-shaped gate by electron beam direct writing, rather complicated processes such as multi-layer resist and/or multi-exposure and development techniques have been required[3].

On the other hand, it is also efficient for reducing the gate resistance to shorten unit gate width using a multi-feed (multi-finger)gate configuration. In the multi-feed gate, the effective gate resistance is in reciprocally proportion to square of the number of gate finger. For example, the effective gate resistance can be reduced by a factor of more than 10 using 14-finger gate compared with that of the practically used π -configuration(4-finger) with equal length(L_g) and total width(W_g).



(a)



(b)

Fig. 1 An SEM photograph (a) and a schematic view (b) of a multi-feed gate HEMT (type-A). The W_a and S_f are the width of air-bridge connection and area of feed-point, respectively

capacitances accurately. The width of the air-bridge connection(W_a) and the size of the feed-point(S_f) are $14\mu m$ and $14 \times 14\mu m^2$, respectively. The epitaxial layers of $n^+ \text{-GaAs}/n\text{-AlGaAs}/i\text{-InGaAs}/i\text{-GaAs}$ for the pseudomorphic HEMT are grown by MBE. About 150nm deep-recess structure is used.

At first, S-parameters of the HEMTs with different number of feeders(N_{fp}) have been measured by on-wafer RF-probing. As the results, we have found that the current gain cut-off frequency(f_T) degrades with increasing the N_{fp} . This suggests that additional parasitic gate capacitances related to the multi-feed configuration degrade the RF performances. The dependence of gate-to-source capacitance(C_{gs}) on the N_{fp} is shown in Fig.2 for the HEMTs with different total-gate-widths(W_g). The C_{gs} is calculated from the measured f_T and transconductance(g_m) using a simple equation of $C_{gs} = g_m / (2\pi f_T)$. The C_{gs} increases linearly with the same slope for each gate-width as the N_{fp} increases. The additional parasitic gate capacitance per a feed-point is estimated to be about $16fF$ from the slope.

In order to clarify the effect of the parasitic gate capacitances on low noise performances, the minimum noise figure(F_{min}) and the associated gain(G_a) of the HEMTs are evaluated at 12GHz as a function of the N_{fp} and the results are shown in Fig.3. The dotted line in the figure is a fitting curve for the F_{min} calculated from the Fukui's equation[4] with only C_{gs} as a fitting parameter. As the curve fits the plotted data well, the degradation of the F_{min} for the N_{fp} s of larger than 3 is concluded to be due to the increase of the parasitic gate capacitances. The improvement of the F_{min} with increasing the N_{fp} up to 3 is thought to be attributed to the reduction of the gate resistance. On the other hand, the G_a decreases linearly with increasing the N_{fp} because of little effect of gate resistance on gain.

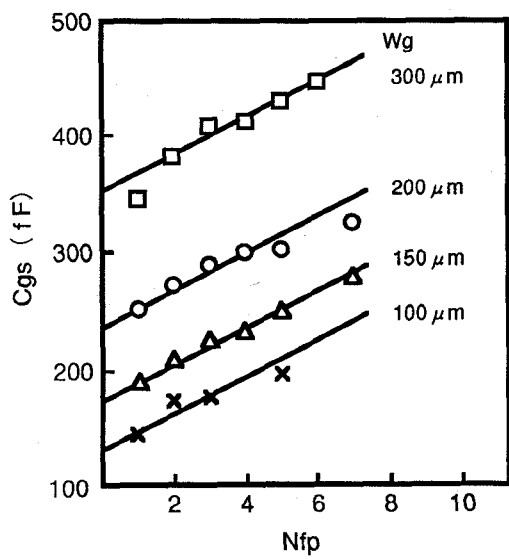


Fig. 2 The dependence of gate-to-source capacitance (C_{gs}) on the number of feed-point (N_{fp}) for different total-gate-widths (W_g).

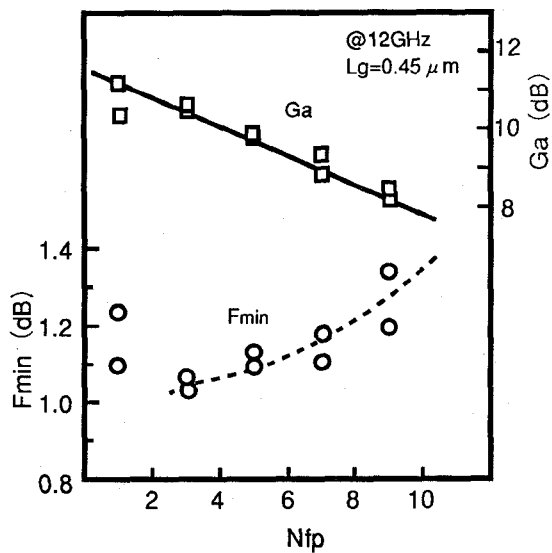


Fig.3 Dependences of minimum noise figure (F_{min}) and associated gain (G_a) on the number of feed-point (N_{fp}).

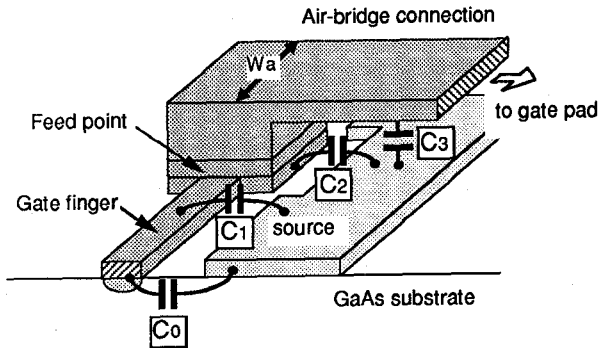


Fig.4 The model of gate-to-source capacitances in the multi-feed gate HEMT.

Table I Gate-to-source capacitances

	C_{gs}	portion
C_0	190 (fF)	60 (%)
C_1	30	10
C_2	50	15
C_3	30	10
other	1	5

$$L_g / W_g = 0.45 / 200 \mu m, N_{fp} = 5$$

To derive some guides to reduce the parasitic gate capacitances related to the multi-feed configuration, we have divided the C_{gs} into the components of C_0 , C_1 , C_2 and C_3 as shown in Fig.4. The C_0 and C_1 are intrinsic and fringing capacitances of the gate finger, and C_2 and C_3 are capacitances related to the feed points and the cross-over parts between the air-bridge connections and the source electrode, respectively. The each component is calculated from the W_g and N_{fp} dependencies of the C_{gs} . Table I summarizes the results for a $L_g/W_g = 0.45/200\mu\text{m}$ and 5-feed(10-finger) HEMT. The $C_2 + C_3$, which is the additional capacitance due to the multi-feed gate configuration, occupies 25% of the total capacitance even in such a long-length($0.45\mu\text{m}$) gate having large C_0 . When the C_0 is reduced by shrinking the gate length, the effect of the $C_2 + C_3$ becomes more serious. Particularly, we should pay attention to the C_2 which is larger than the C_3 . From these investigations, we conclude that it is crucial for reduction of the parasitic gate capacitances to miniaturize not only the width of the air-bridge connection(W_a) but also the area of the feed-point(S_f).

To confirm the effect of miniaturizing the W_a and S_f in the practical quarter-micron gate devices, the S_f dependence of the C_{gs} is examined with the W_a as a parameter for $L_g/W_g = 0.25/200\mu\text{m}$ HEMTs and the results are shown in Fig.5. The C_{gs} is successfully reduced from 280 to 220fF by miniaturizing the W_a/S_f from $14\mu\text{m}/196\mu\text{m}^2$ to $5\mu\text{m}/6\mu\text{m}^2$. It should be noted that the reduction of the C_{gs} is mainly attributed to that of the C_2 by miniaturizing the S_f . Considering that the $C_2 + C_3$ has been 80fF for the W_a/S_f of $14\mu\text{m}/196\mu\text{m}^2$, the residual parasitic gate capacitance related to the configuration is estimated to be about 20fF, which is mainly the capacitance of the cross-over parts (C_3).

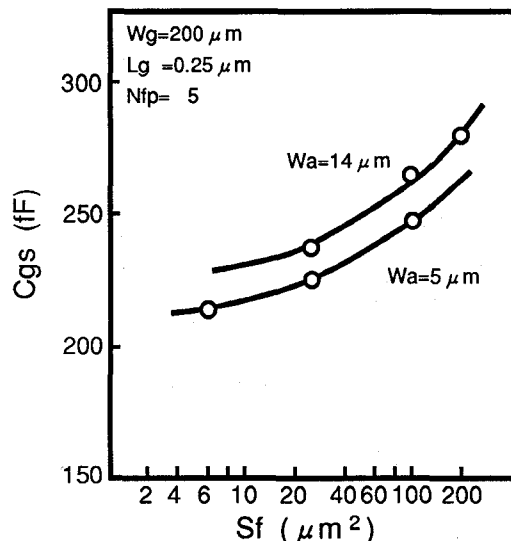
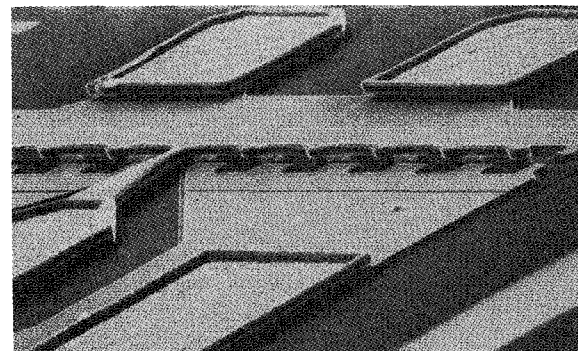


Fig.5 The feed-point area (S_f) dependences of gate-to-source capacitance (C_{gs}) in the HEMTs with air-bridge metallization width (W_a) of 14 and $5\mu\text{m}$.

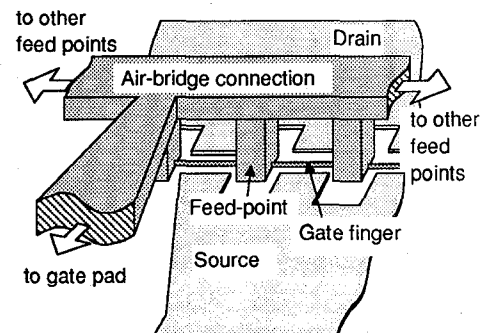
A NOVEL MULTI-FEED GATE CONFIGURATION

In order to reduce the residual parasitic gate capacitance further, we have designed a novel multi-feed gate configuration(type B) as shown in Fig.6, in which the W_a/S_f are also reduced to $5\mu\text{m}/6\mu\text{m}^2$. In the configuration, the feed points are interconnected by an air-bridge formed just above the gate finger so that no air-bridge connection crosses over the source electrode. The dependence of the f_T on the N_{fp} is compared with that of type A in Fig.7. The degradation of the f_T with increasing the N_{fp} is considerably suppressed in type B.

Figure 8 shows the dependencies of both F_{min} and G_a at 12GHz on the N_{fp} in type B HEMTs having $0.25\mu\text{m}$ gate. The F_{min} is decreasing with increasing the N_{fp} up to 11. The curve for the F_{min} in the figure is calculated using the Fukui's equation with fixed parameters except for the gate resistance. The effective gate resistance of the HEMT with 11 feeds, whose unit gate width is as small as $6.8\mu\text{m}$, is approximated to be less than 0.1Ω . Since this curve fits the data well, we can be convinced that the parasitic gate capacitances originated from the multi-feed gate configuration in type B have little effect on the low noise performances.



(a)



(b)

Fig.6 An SEM photograph (a) and a schematic view (b) of a novel multi-feed HEMT (type-B).

The HEMT with 11 feeds shows the best F_{min} of 0.55dB and the associated gain of 10.2dB at 12GHz. The dependence of the F_{min} and the G_a on the drain current(I_{ds}) is shown in Fig.9. At 40GHz, the F_{min} of 1.6dB is also obtained. These low noise performances are satisfactory compared with those of the state-of-the-art T-shaped gate GaAs based HEMTs with the same gate length.

To demonstrate the advantages of the HEMT for MMIC, Q-band low noise MMIC amplifiers using this multi-feed gate configuration have been developed for millimeter-wave communications. In 2-stage amplifier, the noise figure of 4.1dB and the gain of 12.2dB are obtained at 40GHz.

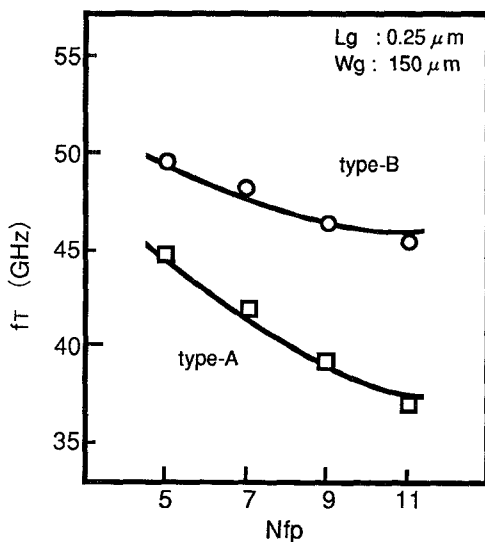


Fig. 7 The number of feed-point (Nfp) dependence of current gain cut-off frequency(f_T) in type-A and B HEMTs.

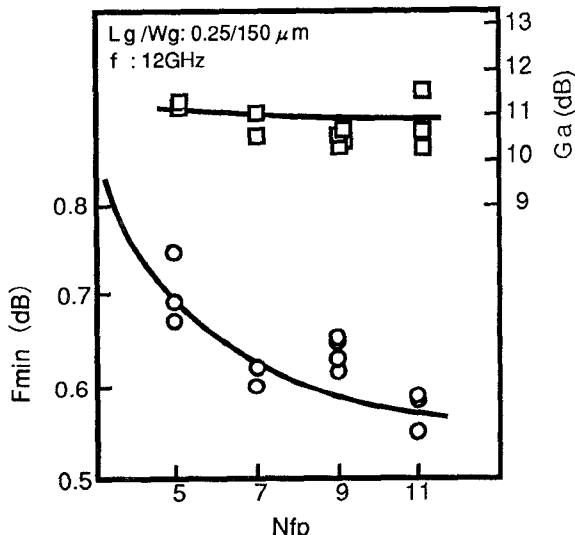


Fig.8 The Nfp dependences of F_{min} and G_a in the type-B HEMTs. The F_{min} curve is fitted using the Fukui's equation with only the gate resistance variable.

CONCLUSIONS

We have realized super low noise HEMTs with a novel multi-feed gate configuration which is designed according to the detailed analysis of parasitic gate capacitances. The minimum noise figures of 0.55 and 1.6dB are achieved for 0.25 μ m gate HEMT at 12 and 40GHz, respectively. Using the multi-feed gate HEMT, low noise 2-stage MMIC amplifiers with the noise figure of 4.1dB and the gain of 12.2dB at 40GHz are also realized.

REFERENCES

- [1] K.H.G.Duh, P.C.Chao, P.Ho, A.Tessmer, S.M.J.Liu, M.Y.Kao, P.M.Smith, and J.M.Ballingall, "W-Band InGaAs HEMT Low Noise Amplifiers," 1990 IEEE MTT-S, p.595, May 1990.
- [2] H.Kawasaki, T.Shino, M.Kawano, and K.Kamei, "Super Low Noise AlGaAs/GaAs HEMT With One Tenth Micron Gate," 1989 IEEE MTT-S, p.423, June 1989.
- [3] P.C.Chao, P.M.Smith, S.C.Palmateer, and J.C.M.Hwang, "Electron-Beam Fabrication of GaAs Low-Noise MESFET's Using a New Trilayer Resist Technique," IEEE Electron Devices, Vol.ED-32, p.1042, 1985.
- [4] H.Fukui, "Optimal Noise Figure of Microwave GaAs MESFET's," IEEE Electron Devices, Vol.ED-26, p.1032, 1979.

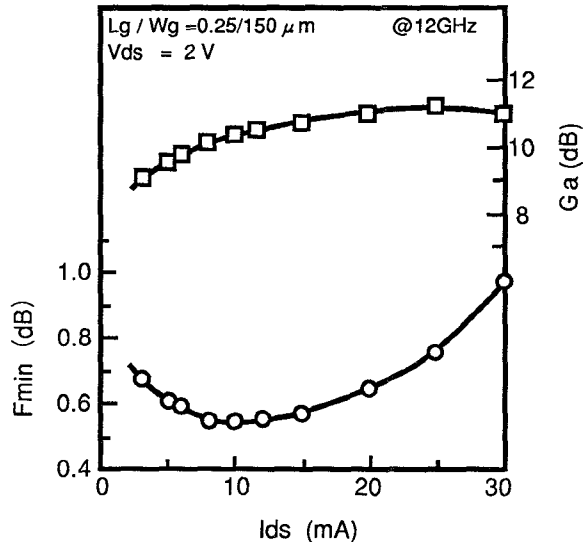


Fig.9 Drain current (I_{ds}) dependences of minimum noise figure(F_{min}) and associated gain(G_a).